

1 **Technical Note: Stability of tris pH buffer in artificial seawater**  
2 **stored in bags**

3 Wiley H. Wolfe<sup>1</sup>, Kenisha M. Shipley<sup>1</sup>, Philip J. Bresnahan<sup>2</sup>, Yuichiro Takeshita<sup>3</sup>, Taylor Wirth<sup>1</sup>,  
4 Todd R. Martz<sup>1</sup>

5 <sup>1</sup>Scripps Institution of Oceanography, University of California San Diego, La Jolla, 92093, USA

6 <sup>2</sup>Department of Earth and Ocean Sciences, University of North Carolina Wilmington, Wilmington, 28403, USA

7 <sup>3</sup>Monterey Bay Aquarium Research Institute, Moss Landing, 95093, USA

8 *Correspondence To:* Philip J. Bresnahan Jr. (bresnahanp@uncw.edu)

9

10 **Abstract**

11 Equimolar tris (2-amino-2-hydroxymethyl-propane-1,3-diol) buffer in artificial seawater is a well characterized  
12 and commonly used standard for oceanographic pH measurements. We evaluated the stability of tris pH when stored  
13 in purportedly gas impermeable bags across a variety of experimental conditions, including bag type, and storage in  
14 air vs. seawater over 300 days. Bench-top spectrophotometric pH analysis revealed that the pH of tris stored in bags  
15 decreased at a rate of  $0.0058 \pm 0.0011 \text{ yr}^{-1}$  (mean slope  $\pm$  95% confidence interval of slope). The upper and lower  
16 bounds of expected pH change at t = 365 days, calculated using the averages and confidence intervals of slope and  
17 intercept of measured pH change vs. time data, were -0.0042 and -0.0076 from initial pH. Analyses of total dissolved  
18 inorganic carbon confirmed that a combination of CO<sub>2</sub> infiltration and/or microbial respiration led to the observed  
19 decrease in pH. Eliminating the change in pH of bagged tris remains a goal, yet the rate of pH change is lower than  
20 many processes of interest and demonstrates the potential of bagged tris for sensor calibration and validation of  
21 autonomous in situ pH measurements.

Deleted:

Deleted:

22 **1. Introduction**

23 Ocean pH is a key measurement used for tracking biogeochemical processes such as photosynthesis,  
24 respiration, and calcification (Takeshita et al., 2016); and represents perhaps the most recognized variable associated  
25 with ocean acidification (OA), the decrease in ocean pH due to the uptake of anthropogenic carbon dioxide (Doney et  
26 al., 2009). OA progresses with a global average pH decline of 0.002 per year in the surface open ocean (Bates et al.,  
27 2014), and the accumulated and projected near-term effects of OA have been shown to have deleterious effects on  
28 many calcifying organisms (Cooley and Doney, 2009). Beyond the narrow scope of calcifiers, organismal response is  
29 complex, exhibiting varied responses across processes such as reproduction, growth rate, and sensory perception.  
30 Organismal responses are further complicated by their impact on ecosystem level dynamics, such as altering  
31 competition and predator-prey relationships (Doney et al., 2020). Furthermore, pH effects are often exacerbated by  
32 concomitant stressors, such as decreased dissolved oxygen or increased temperature. Ultimately, OA will affect  
33 humans through impacts on fisheries, aquaculture, and shoreline protection (Branch et al., 2013; Doney et al., 2020).

34 The quality of pH measurement required to observe various phenomena is often broken into “climate” and  
35 “weather” levels of uncertainty (Newton et al., 2015), or 0.003 and 0.02, respectively. Discrete sampling has been  
36 shown to be capable of meeting the climate level of uncertainty when best practices are followed, yet many labs do  
37 not consistently meet this standard (Bockmon and Dickson, 2015). Furthermore, while discrete, bench-top  
38 methodologies can be the most accurate, the ocean’s vast size limits the oceanographic community’s ability to make  
39 ship-based discrete pH measurements to decadal reoccupations of a few major sections per ocean basin (Sloyan et al.,  
40 2019). The sparsity of ship-board measurements hinders our ability to assess sub-decadal processes, such as seasonal  
41 cycles or bloom events, over much of the ocean (Karl, 2010), and highlights the need for autonomous, high-frequency  
42 pH measurements. Technological advancements have led to more routine autonomous pH measurements over the past  
43 decade, providing opportunities to fill some gaps in time and space in discrete sampling programs (e.g. Byrne, 2014;  
44 Martz et al., 2015; Lai et al., 2018; Wang et al., 2019; Tilbrook et al., 2019). Globally, pH sensors now operate on

47 hundreds of autonomous platforms including moorings and profiling floats, delivering unique datasets in the form of  
48 Eulerian and depth resolved Lagrangian time series (Johnson et al., 2017; Bushinsky et al., 2019; Sutton et al., 2019).  
49 While sensors increase data coverage, many sensor-based pH measurements, particularly on moored systems, continue  
50 to fall short of both climate and weather levels of uncertainty, as highlighted in the intercomparison tests carried out  
51 by the Alliance for Coastal Technologies (ACT, 2012) and by the Wendy Schmidt Ocean Health XPRIZE (Okazaki  
52 et al., 2017).

53 Independent validation is typically required for autonomous sensors to meet both weather and climate levels  
54 of uncertainty. For example, autonomous underway  $p\text{CO}_2$  systems (Pierrot et al., 2009), moorings (Bushinsky et al.,  
55 2019), and autonomous surface vehicles (Chavez et al., 2017; Sabine et al., 2020) are able to provide climate quality  
56 observations with an uncertainty of  $\pm 2 \mu\text{atm}$  because traceable standard gases are frequently measured in situ. For pH  
57 measurements on profiling floats (Johnson et al., 2016), sensor performance is validated by comparing to a deep  
58 reference pH field that is calculated using empirical algorithms (Williams et al., 2016; Bittig et al., 2018; Carter et al.,  
59 2018). This approach has demonstrated the ability to obtain high quality pH measurements from a network of profiling  
60 floats (Johnson et al., 2017) but requires measurements in the deep ocean where pH is comparatively stable. It is  
61 atypical for other pH sensors, including coastal moored sensors, to have an automated or remote validation. Therefore,  
62 on such deployments, validation has largely relied on discrete samples taken alongside the sensor (Bresnahan et al.,  
63 2014; McLaughlin et al., 2017; Takeshita et al., 2018), which presents unique challenges; primarily that spatiotemporal  
64 discrepancy can lead to errors of  $> 0.1$ , especially in highly dynamic systems (Bresnahan et al., 2014).

65 Similar to the method in use by  $p\text{CO}_2$  systems, one approach to validate in situ pH sensors is by measuring a  
66 reference material or pH standard, repeatedly during a sensor deployment. The most commonly used standard for  
67 oceanographic pH measurement is equimolar tris (2-amino-2-hydroxymethyl-propane-1,3-diol) buffer in artificial  
68 seawater (ASW), hereafter referred to as tris or tris-ASW (DelValls and Dickson, 1998; Papadimitriou et al., 2016).  
69 The pH of tris has been characterized over a range of temperature, salinity, and pressure (DelValls and Dickson, 1998;  
70 Rodriguez et al., 2015; Takeshita et al., 2017; Müller et al., 2018), allowing for accurate calculation of tris pH across  
71 a wide range of marine conditions. Furthermore, when stored in borosilicate bottles and under ideal conditions, these  
72 buffers have been shown to be stable to better than 0.0005 over a year (Dickson, 1993; Nemzer and Dickson, 2005),  
73 making tris a good candidate for in situ validation of long-term deployments of autonomous pH sensors. To be utilized  
74 for in situ applications, the reference solution must be stored in bags (as in, Hales et al., 2005; Seidel et al., 2008;  
75 Sayles and Eck, 2009; Spaulding et al., 2014; Wang et al., 2015; Lai et al., 2018). Recently, in situ sensor validation  
76 using bagged tris was demonstrated by Lai et al. (2018) during a 150-day deployment of an autonomous pH sensor,  
77 where the tris standard was measured in situ every 5 days. However, the stability of tris when stored in bags has not  
78 been quantified systematically using spectrophotometric bench-top pH measurement techniques recommended as best  
79 practices (Dickson et al., 2007).

80 In this work we quantified the stability of tris stored in bags for 300 days. Tris from four separately prepared  
81 batches was stored in two bag types either in a lab or submerged in seawater. In addition, one batch was stored in  
82 borosilicate bottles in the lab as a control. Spectrophotometric pH measurements were made approximately every two

83 months on each bag of tris. Throughout the experiment, Certified Reference Materials (CRMs) for oceanic CO<sub>2</sub>  
84 measurements (Dickson, 2001) were used to assess the stability of the spectrophotometric pH system.

## 85 2. Methods

86 Two bag types were tested for storing tris (Figure 1). Bag type 1 was custom made based on a design used in  
87 the “Burke-o-Lator” system (Hales et al., 2005; Bandstra et al., 2006), made from PAKDRY 7500 barrier film  
88 (IMPAK P75C0919). The barrier film is made of layers of polyester and nylon with a sealant layer of metallocene  
89 polyethylene. Two 23 x 48 cm (9” x 19”) sheets were heat sealed on three sides, forming a pocket, and a 1.9 cm (3/4”)  
90 diameter hole was cut into one of the pocket walls for the bulkhead fitting and bulkhead nut (McMaster-Carr  
91 8674T55). The bulkhead was sealed into the wall with a silicone gasket (McMaster-Carr 9010K13), washer  
92 (McMaster-Carr 95649A256), and coated with silicone sealant (McMaster-Carr 74955A53). A “push-to-connect” ball  
93 valve fitting (McMaster-Carr 4379K41), was attached to the bulkhead. The modified pocket was rinsed, dried, and  
94 heat sealed along the final edge to create a ~4 L bag. Bags were left to dry for at least 24 hours before filling. Bag type  
95 2 was a commercially available 3 L Cali-5-Bond bag purchased from Calibrated Instruments and used without  
96 modification. It is a multi-layer bag made of plastic, aluminium foil (to prevent liquid and gas permeation), a layer of  
97 inert high density polyethylene (to form a non-reactive inner wall) and, a polycarbonate Stopcock Luer valve.

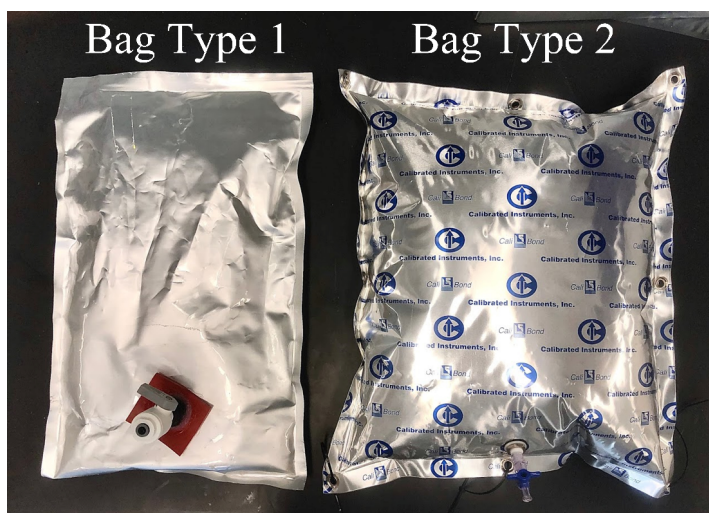


Figure 1: A picture of bag type 1 and 2 used to store tris in this study.

98 In this experiment, four batches of tris were prepared following the procedure in DelValls and Dickson  
99 (1998), using off-the-shelf reagents with no additional standardization or purification (e.g. recrystallization of salts).  
100 The focus of this paper is stability of bagged tris over time and does not prioritize obtaining highly accurate equimolar  
101 tris (as would be necessary for characterization of thermodynamic constants, for example). The calculated pH of tris

102 in this study was 8.2652 at 20°C, based on quantity of reagents used. This is 0.0135 higher than the pH of equimolar  
 103 tris, 8.2517 at 20°C (DeValls and Dickson, 1998). The pH discrepancy was due to a unit error in the measurement of  
 104 HCl (our preparation used mol/L rather than the prescribed mol/kg-sol). This unit error resulted in a tris:trisH<sup>+</sup> of  
 105 1:0.97 that slightly differs from the 1:1 of truly equimolar tris. As this ratio is nearly equimolar, the term “equimolar”  
 106 will continue to be used throughout this study. The details of the specific reagents used to prepare the tris solution can  
 107 be found in Table A1.

108 Three stability tests were initiated at different times over the course of 18 months. The initiation of a given  
 109 test is defined as the date of preparation of the tris used in that test. A summary of the differences between these tests  
 110 is shown in Table 1 and described here. Each bag has a unique identifier in the format of “Batch #, Bag #, Lab or  
 111 Tank.” If this identifier is duplicative, the bags are differentiated with letters A to D. Each bag was rinsed before  
 112 filling: 3 times with deionized water (DI), 5 times with ultrapure water (> 18 MΩ resistivity) and at least 3 times with  
 113 200 mL of tris. Tris bags were stored on a lab bench or in a 5,000 L test tank filled with ozone-sterilized, filtered  
 114 seawater. Bag type 2 experienced delamination of exterior layers when stored in seawater during test 2 and was not  
 115 used in further testing. Tris from batch 4 was also stored in borosilicate bottles following the procedure in Nemzer  
 116 and Dickson (2005). In addition to pH measurements, dissolved inorganic carbon (C<sub>T</sub>) was measured on both bagged  
 117 and bottled tris during test 3 to see if changes in pH were due to increased CO<sub>2</sub>. C<sub>T</sub> samples were measured using a  
 118 custom-built system based on an infrared (IR) analyser (LI-COR 7000) similar to systems used by O’Sullivan and  
 119 Millero (1998) and Friederich et al. (2002). This IR measurement system is capable of measuring relatively low C<sub>T</sub>  
 120 without requiring method adjustment and has been used to make near zero C<sub>T</sub> measurements (Paulsen and Dickson,  
 121 unpublished data). C<sub>T</sub> measurements were made on CRMs (Batch 179 & 183). The precision of the C<sub>T</sub> measurements  
 122 was ± 1.4 µmol/kg (pooled standard deviation, n<sub>samples</sub>=15, n<sub>measurements</sub>=44).

123 **Table 1: Tris preparation and storage.**

	Bag Type	Tris Batch	Date Made	Storage Location	Rinse Procedure	C <sub>T</sub> Measured
Test 1	1 & 2	1 & 2	13 Dec 2017	Lab & Tank	3x DI, 5x ultrapure, 3x tris	No
Test 2	1 & 2	3	13 April 2018	Lab & Tank	3x DI, 5x ultrapure, 3x tris	No
Test 3	1 & bottle	4	26 February 2019	Lab	3x DI, 5x ultrapure, ≥ 6x tris	Yes

124  
 125 Tris pH was measured every 55 ± 20 days (mean ± standard deviation of measurement interval) throughout  
 126 the experiment. The pH of tris was measured in triplicate at each time point with spectrophotometry using m-cresol  
 127 purple as the indicator dye using the system described in Carter et al. (2013). Absorbance measurements were made  
 128 in a 10-cm jacketed cell, and the temperature was measured directly adjacent to the cell outflow using a NIST-traceable  
 129 thermometer (± 0.1 °C, QTI DTU6028P-001-SC). Blank and sample were held for 3 minutes in the jacketed flow cell  
 130 prior to absorbance measurements.

131 On average, temperature was stable to within a 0.02 °C range over the course of the day; the mean temperature  
 132 throughout the experiment was  $20.09 \pm 0.23$  °C (1  $\sigma$ ), although temperature was 0.6 °C higher than the average on  
 133 one measurement day. Spectrophotometric pH measurements are reported at 20 °C by adjusting the measured pH  
 134 value at the measured cell temperature  $T_C$  ( $pH_{spec,T_C}$ ) to 20 °C ( $pH_{spec,20^\circ C}$ ) using the known temperature dependence  
 135 of tris ( $pH_{tris}$ ) as follows:

$$pH_{spec,20^\circ C} = pH_{spec,T_C} - (pH_{tris,T_C} - pH_{tris,20^\circ C}) \quad (1)$$

136  $pH_{tris,T_C}$  and  $pH_{tris,20^\circ C}$  are the theoretical pH of tris (at the measured temperature and 20 °C respectively) and were  
 137 calculated using Eq. (18) in DelValls and Dickson (1998). This adjustment assumes that any potential difference in  
 138  $\partial pH/\partial T$  between that corresponding to equimolar tris and that corresponding to our 1:0.97 tris:trisH<sup>+</sup> ratio has a  
 139 negligible effect over the small temperature range observed.

140 To account for pH-dependent errors from impurities in unpurified mCP, a pH-dependent correction factor  
 141 was determined based on the protocol outlined in Takeshita et al. (*in review*). Briefly, pH of natural seawater with  
 142 different ratios of added tris:trisH<sup>+</sup> was measured subsequently using impure dye ( $pH_{impure}$ ; from Aldrich, lot  
 143 MKBH6858V) and purified dye ( $pH_{pure}$ ; from Robert Byrne's Laboratory, University of South Florida (Liu et al.,  
 144 2011)) over a range of pH between 7.4 to 8.2 at approximately 0.2 intervals. Varying ratios of tris:trisH<sup>+</sup> were used to  
 145 obtain different solution pH, and to buffer any changes in pH during the experiment, which negates the need for dye  
 146 perturbation corrections in this characterization. Triplicate measurements were made at each pH. A second order pH-  
 147 dependent error was observed as previously described, following the equation ( $R^2 = 0.975$ , RMSE = 0.000434):

$$pH_{pure} = -0.0047777 \times pH_{impure}^2 + 1.0668875 \times pH_{impure} - 0.2359740 \quad (2)$$

148 All subsequent  $pH_{spec}$  measurements in this study were conducted with impure dye and are reported with this dye  
 149 impurity correction (Eq. 2) applied. The correction adjusted the reported pH by  $0.0093 \pm 0.0002$  (mean  $\pm$  standard  
 150 deviation,  $n = 126$ ). No dye perturbation correction was used (a correction for a change in pH caused by the addition  
 151 of the dye). As the high buffering capacity of tris, in combination with a dye adjusted to a pH similar to that of tris,  
 152 results in a negligible change in measured pH.

153 Measurements of tris batches 1 and 2 made in the first 150 days have been removed from the data set due to  
 154 procedural changes made to the spectrophotometric pH system to correct for problems with temperature equilibration.  
 155 Outliers were removed from the spectrophotometric pH measurements if the absorbance at 760 nm was above 0.005  
 156 or below -0.002 (indicative of a measurement problem, such as a bubble or lamp drift), resulting in the removal of 2  
 157 out of 163 measurements. Additionally, outliers were removed from the data set if they were greater than three  
 158 standard deviations from the mean of a measurement triplicate, where standard deviation is calculated as using all sets  
 159 of triplicates (1 standard deviation = 0.0004,  $n = 55$ ), resulting in the removal of 2 of 161 remaining measurements.  
 160 The remaining 159 measurements were used for the analysis presented here. An analysis of variation, or ANOVA,  
 161 was used to detect the dependence of the results on tris batch, bag/bottle type and storage location. Analysis was  
 162 performed using MATLAB R2020a and the standard function "anovan()." Throughout the experiment, CRMs  
 163 (procured from A. Dickson, Scripps Institution of Oceanography) for seawater  $C_T$  and total alkalinity were measured  
 164 regularly to verify instrument performance (Dickson, 2001). A time-series of CRM measurements over the duration  
 165 of the work described here showed no systematic drift. (Fig. A1 in Appendix A). To assess if the change in pH was

Deleted: review

Deleted: addedseawater

Deleted: Lab

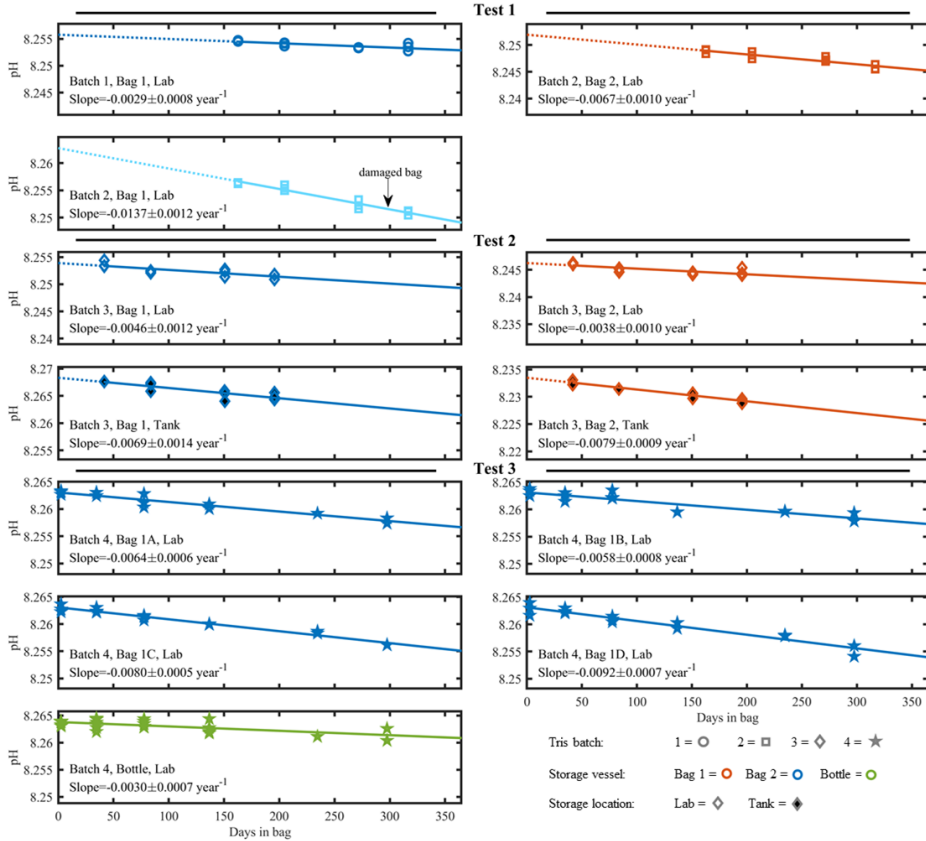
169 driven by the addition of CO<sub>2</sub>, the final pH and available C<sub>T</sub> measurements were compared with a model described  
170 here. The theoretical change in tris-artificial seawater (ASW) pH due to an increase in C<sub>T</sub> is straightforward to  
171 calculate, since both tris and CO<sub>2</sub> acid-base equilibria are well-characterized in seawater and ASW media. The pH is  
172 calculated for tris-ASW + C<sub>T</sub> using an equilibrium model following the approach described in Chapter 2 of Dickson  
173 et al. (2007) for the case of known alkalinity and C<sub>T</sub>. In the case of ASW, the seawater equilibrium constants for CO<sub>2</sub>  
174 are appropriate because minor ions present in seawater and not ASW do not appreciably affect the CO<sub>2</sub> equilibrium  
175 constants (particularly when the goal is to compute relative changes in pH) as the ionic background of ASW is closely  
176 matched to that of seawater at salinity = 35. In our model, minor acid-base species important to seawater alkalinity  
177 but not present in ASW (borate, phosphate, silicate, fluoride) are set to zero. The definition of total alkalinity is  
178 modified to include the tris acid-base system following the definition of acid-base donor/acceptor criteria given by  
179 Dickson (1981): tris is assigned as a level-1 proton acceptor and tris-H<sup>+</sup> is at the zero level. Thus, in our model, tris<sub>tot</sub>  
180 = 0.08 molal and alkalinity = 0.04 molal and C<sub>T</sub> is a variable. An algorithm (see Annexe 1 in Dickson et al. (2007)) is  
181 then used to find the root of the alkalinity equation in its residual form by solving for pH.

### 182 3. Results & Discussion

183 **Figure 2** depicts pH<sub>spec,20°C</sub>, stored in either a bag or bottle, as a function of time and is subdivided for tests 1,  
184 2, and 3. A linear decrease was observed for all bags or bottles. A linear regression was calculated for each  
185 experimental condition and, in the cases where measurements at t = 0 were removed due to protocol changes described  
186 above, the line was extrapolated back to t = 0, shown by the dotted line. The measured or extrapolated y-intercept is  
187 reported as the initial pH in Table 2. In all tests, trendlines are extrapolated to t = 365 days to illustrate observed and

Deleted: Figure 2

189 predicted change over the course of a year as shown by the solid line. For ease of visual comparison, the y-axis of  
 190 each subplot has an identical pH range of 0.017.  
 191



192  
 193 **Figure 2: Individual time series of measured pH in tris buffer solutions. Tris batch is indicated by shape, storage vessel by**  
 194 **color, and storage location by fill. This marker system is also followed in Fig. A2. The solid line is a linear regression starting**  
 195 **at the first included pH measurement and ending 365 days after the tris was bagged. The dotted line illustrates the**  
 196 **extrapolation back to 0 days stored in bag when measurements at t = 0 do not exist. The range of the y-axis scale is fixed at**  
 197 **0.017 pH for all subplots.**

198

**Deleted:** Bag type 1 is shown in blue (light blue for the damaged bag of type 1), 2 in orange and bottle in green. Tris batch 1 is depicted as circles, 2 as squares, 3 as diamonds and 4 as stars. Storage location in tank has a black fill and lab symbols have no fill. ...

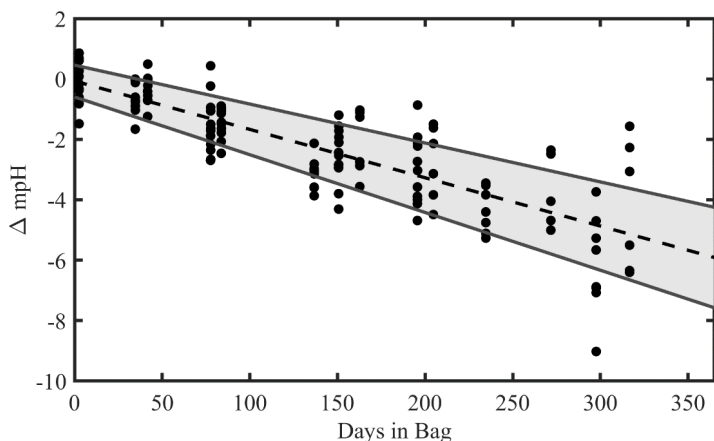


204 **Table 2: Linear regression statistics from trendlines shown in Fig. 1 and 2. The last row shows the regression statistics for**  
 205 **tris from all batches, in either bag type, stored in the lab or test tank. Slope and intercept are shown as mean  $\pm$  95%**  
 206 **confidence intervals. The reported intercept is the regression intercept; when initial pH measurements are available, they**  
 207 **differ by less than 0.0003 from regression intercept. \* Indicates the outlier (Batch 2, Bag 1, Lab) caused by a damaged bag.**  
 208 **The outlier, “Batch 2, Bag 1, lab”, was not used in the “All Batches, All Bags, Lab or Tank” composite. † In all batches, all**  
 209 **bags, lab or tank, the slope was calculated with a linear fit of all (non-outlier) tris measurements. The RMSE is the mean**  
 210 **RMSE of all (non-outlier) bag fits. ‡ The calculated tris pH was calculated at 20°C; however, this calculated pH is 0.0135**  
 211 **higher than equimolar tris as noted above (DeValls and Dickson, 1998).**

Batch & Storage Method	Slope (mPH yr <sup>-1</sup> )	Intercept (Initial pH)	RMSE (mPH)	r <sup>2</sup>	n
Batch 1, Bag 1, Lab	-2.9 $\pm$ 1.7	8.2558 $\pm$ 0.0012	0.43	0.59	12
Batch 2, Bag 1, Lab*	-13.7 $\pm$ 2.7	8.2627 $\pm$ 0.0018	0.61	0.94	11
Batch 2, Bag 2, Lab	-6.7 $\pm$ 2.2	8.2519 $\pm$ 0.0015	0.55	0.82	12
Batch 3, Bag 1, Lab	-4.6 $\pm$ 2.7	8.2539 $\pm$ 0.0010	0.62	0.62	11
Batch 3, Bag 1, Tank	-6.9 $\pm$ 3.2	8.2683 $\pm$ 0.0012	0.73	0.73	11
Batch 3, Bag 2, Lab	-3.8 $\pm$ 2.1	8.2462 $\pm$ 0.0008	0.54	0.61	12
Batch 3, Bag 2, Tank	-7.9 $\pm$ 2.1	8.2335 $\pm$ 0.0008	0.44	0.92	9
Batch 4, Bag 1A, Lab	-6.4 $\pm$ 1.3	8.2630 $\pm$ 0.0005	0.64	0.90	14
Batch 4, Bag 1B, Lab	-5.8 $\pm$ 1.8	8.2631 $\pm$ 0.0008	0.91	0.79	15
Batch 4, Bag 1C, Lab	-8.0 $\pm$ 1.0	8.2631 $\pm$ 0.0004	0.49	0.96	15
Batch 4, Bag 1D, Lab	-9.2 $\pm$ 1.6	8.2631 $\pm$ 0.0007	0.80	0.92	15
Batch 4, Bottle, Lab	-3.0 $\pm$ 1.4	8.2638 $\pm$ 0.0005	0.81	0.44	25
All Batches, All Bags, Lab or Tank†	-5.8 $\pm$ 1.1	–	0.72	0.66	126
Calculated tris pH‡	–	8.2652	–	–	–

212  
 213 Only bags from test 3, using tris batch 4 and bag type 1, have direct initial pH measurements and replicate  
 214 bags. Initial pH measurements of these 4 bags were 8.2630  $\pm$  0.0007 (mean  $\pm$  standard deviation, n = 12). Importantly,  
 215 the very low standard deviation suggests that a single initial pH measurement is representative of all replicate bags  
 216 filled with a single tris batch, if the preparation procedure used in test 3 is followed. This inter-bag consistency is  
 217 beneficial because it reduces the number of initial pH measurements required when filling multiple bags. There is also  
 218 strong agreement in initial pH measurements between bagged and bottled tris in test 3, with the initial pH of bottled  
 219 tris 0.0007 higher than bagged tris (8.26327  $\pm$  0.0004, n = 6). The differences in filling procedure or impurities between  
 220 bags and bottles in test 3 appear to have little effect on the initial pH. The mean initial pH of tris batch 4 is 0.002 (n =  
 221 5) lower than calculated pH<sub>tris,20°C</sub> (Fig. A2). This difference between the mean initial pH of tris batch 4 and calculated  
 222 pH<sub>tris,20°C</sub> is similar in direction and magnitude to those reported in other studies: DeGrandpre et al. (2014) reported –  
 223 0.0012  $\pm$  0.0025 and Müller and Rehder (2018) reported -0.002 to -0.008 (measured pH minus pH<sub>tris,Tc</sub>). With standard  
 224 laboratory equipment and off-the-shelf reagents, an uncertainty of 0.006 is expected in prepared tris (Paulsen and  
 225 Dickson, 2020). Measurements were also made on Dickson standard tris (batch T35) using the same instrument and  
 226 the pH was 0.0019 higher than the calculated pH<sub>tris,20°C</sub> (n = 2). In tests 1 and 2, the initial pH was extrapolated from  
 227 a linear regression. The extrapolated initial pH values are more variable and lower (on average) than those directly

228 measured (Fig. A2). These differences may be a result of the extrapolation or different experimental variables such as  
 229 the increased rinsing of bags, or the single bag type and storage location used in test 3.



230

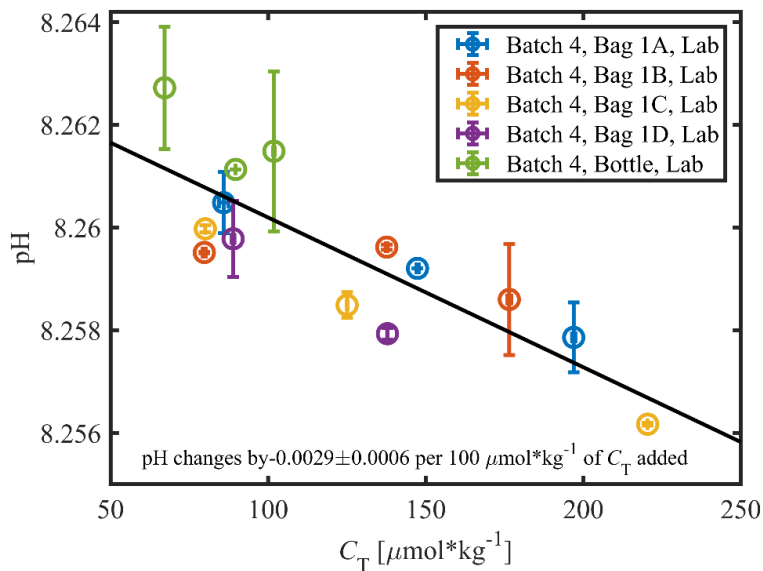
231 **Figure 3: Combined time series of measured pH in tris buffer tris buffer solutions. The dots represent every**  
 232 **measurement made on a (non-damaged) bag of tris. The dotted line is the “All Bags, All Batches, Lab or Tank”**  
 233 **regression. The grey shaded region is the observational 95% confidence interval (CI). The CI is intended to**  
 234 **estimate the future pH of a tris bag (with known initial pH and an unmeasured bag specific rate of change).**  
 235 **The upper and lower bounds are -0.0042 and -0.0076 pH per year, respectively.**

236 Figure 3 depicts a composite of all test results as the change from the initial pH of tris  
 237 ( $\Delta pH = pH_{spec,20^\circ C}^{t=day} - pH_{spec,20^\circ C}^{t=0}$ ) as a function of time elapsed since bagging. A linear regression on all pH  
 238 measurements, excluding the outlier of “Batch 2, Bag 1, Lab”, of tris stored in bag types 1 or 2, has a slope of  $-0.0058$   
 239  $\pm 0.0011 \text{ yr}^{-1}$  (mean  $\pm$  95% C.I.). The upper and lower bounds of  $\Delta pH$  at  $t = 365$  days,  $-0.0042$  and  $-0.0076$ , are  
 240 important to consider when utilizing this bagged storage method of tris. These bounds provide the broadest expected  
 241 range in pH change over a year of storage, and include both the intercept and slope confidence intervals (*slope<sub>CI</sub>* and  
 242 *intercept<sub>CI</sub>*, respectively). For example, the upper bound of  $\Delta pH$  at  $t = 365$  days is calculated as: *upper bound =*  
 243 *(slope + slope<sub>CI</sub>) \* 365 + intercept + intercept<sub>CI</sub>*. The outlier (Batch 2, Bag 1, Lab) was excluded due to  
 244 noticeable damage to the bag (see Fig. A3 in Appendix A), which is believed to have caused its pH to decrease at  
 245 more than two times the average rate of the other bags. The damage appears to be a break in the metallic bag layer,  
 246 potentially caused by creasing or pinching of the bag when handling. This observation highlights the importance of  
 247 maintaining bag integrity, particularly during use in the field. A successful two-week field deployment has been  
 248 conducted using the tris bags described here and a modified SeapHOx in a shallow, coral reef flat (Bresnahan et al.  
 249 2021). This two-week deployment was significantly shorter than the year of storage described here and further field  
 250 testing in longer deployments in varied environments are required before widespread use of this technology. For the  
 251 longer time frame depicted in Figure 3, the only comparable example found in the literature is the work of Lai et al.

- Deleted: ,
- Formatted: Font: Italic
- Formatted: Font: Italic, Subscript
- Formatted: Font: Italic
- Formatted: Font: Italic, Subscript
- Deleted: ,

254 (2018). In this work, Lai et al. (2018) used bagged tris for sensor calibration, with in situ tris measurements made over  
 255 150 days. Lai et al. (2018) did not report a change in the pH of bagged tris over the deployment; however, the reported  
 256 precision of the SAMI-pH in situ instrument ( $\pm 0.003$ ) would not resolve the expected change shown in our Figure 3.  
 257 Therefore, the results of Lai et al. (2018) are not inconsistent with our study.

258 A significant increase in  $C_T$  was observed for all types of bags and bottles in Experiment 3 (Figure 4). A high  
 259 correlation between solution pH and  $C_T$  was observed, with a slope of  $-0.0029 \pm 0.0006$  pH per  $100 \mu\text{mol kg}^{-1}$  ( $n =$   
 260  $14$ ,  $r^2 = 0.70$ ), suggesting that the change in tris pH and  $C_T$  was primarily driven by an increase in  $\text{CO}_2$ . The observed  
 261 slope agrees closely with a theoretical model prediction of a linear decrease in pH of  $-0.0024$  per  $100 \mu\text{mol kg}^{-1}$  of  
 262  $C_T$  added (over the range of  $C_T$  observed). There are two possible sources of the increasing  $C_T$ : gas exchange of  $\text{CO}_2$   
 263 with the environment and microbial respiration within the storage vessel. Gas exchange should not be a significant  
 264 source of  $\text{CO}_2$  for tris stored in a borosilicate bottle, as this is the standard equipment used to store seawater  $\text{CO}_2$  and  
 265 tris buffers and is known to minimize gas exchange (Dickson et al. 2007). Therefore, it is likely that respiration was  
 266 the primary driver for the increase in  $C_T$  for tris stored in bottles. On average, pH decrease of tris stored in bags was  
 267 larger than that in the standard bottle (Figure 2), indicating either an additional source of  $\text{CO}_2$  from gas exchange, or  
 268 larger amounts of respiration. Distinguishing between these two theorized sources would require measurements of  
 269 additional parameters such as dissolved organic carbon.



270  
 271 **Figure 4: pH plotted against  $C_T$  shows a linear relationship between the two parameters in tris buffer with a slope of  $-$**   
 272  **$0.0029$  pH for every  $100 \mu\text{mol kg}^{-1}$  of  $C_T$  added. The measurements shown are from three sampling occurrences between**  
 273 **130–300 days stored on bags and bottles used in Test 3. Only two measurements are shown for “Batch 4, Bag 1D, Lab”**  
 274 **because it ran empty before  $C_T$  were made.**

275 The pH stability of tris could be improved by reducing either likely source of  $C_T$ : gas exchange or microbial  
276 respiration. For bags,  $CO_2$  may diffuse through the fittings, gasket, or bag walls, particularly if damaged. The relatively  
277 small breaks in the aluminium foil layer caused “Batch 2, Bag 1, Lab” to decrease more than twice as fast as the  
278 average bag. Storage bag, fitting, and gasket material, as well as careful handling, are therefore important factors in  
279 minimizing gas exchange. For example, silicone is permeable to  $CO_2$ , and thus could have been a path of gas exchange  
280 into the tris for this experiment. As noted above, Nemzer and Dickson (2005) found an almost negligible change of  
281  $0.5 \text{ mpH yr}^{-1}$  in bottled tris. Our bottled tris changed at  $-3.0 \text{ mpH yr}^{-1}$  ( $n = 10$  bottles measured over 161 days),  
282 approximately half the rate of the tris stored in bags. While  $-3.0 \text{ mpH yr}^{-1}$  is near the detection limit of our  
283 measurements, it suggests that the bottling protocol used in this study was not as well controlled as that of Nemzer  
284 and Dickson (2005). For example, the Dickson lab at Scripps Institution of Oceanography regularly uses an annealing  
285 oven to combust all trace organic films that may persist on glass bottles, but in our study, bottles were not annealed.  
286 Although bags cannot be annealed, future steps that may be worth consideration to reduce microbial respiration in  
287 bags include addition of a biocide to the tris solution, acid cleaning the bags, and using ultraviolet light to remove  
288 organics from the ultrapure water used to prepare tris. There are some disadvantages to these proposed steps. Addition  
289 of a biocide may not be ideal for use in sensitive environments if the tris is discharged after use and would alter the  
290 composition of the solution slightly. While rinsing or prolonged soaking of the bags with an acid may help to remove  
291 organics, it is unclear if it would have negative effects on the integrity of the bags. Beyond removing organics on the  
292 bag surfaces, care should be taken to avoid introducing organic contaminants into the tris during the solution  
293 preparation and bag filling procedures to minimize future respiration.

294 Both bag type 1 and 2 experienced problems with structural integrity during this experiment. A single type 2  
295 bag experienced delamination of exterior bag layers when stored submerged in seawater, causing the eventual tearing  
296 and failure of the bag when handling. Bag type 2 was not used in test 3 due to this failure. It should be noted that in  
297 other studies which successfully used bag type 2, the bag was submerged in seawater for less time than in this  
298 experiment (Sayles and Eck, 2009; Aßmann et al., 2011; Wang et al., 2015). A single bag type 1 had the subtler  
299 problem of small breaks in the aluminium foil bag layer, likely causing an increased pH rate of change. In non-  
300 damaged bags, factors such as bag type/bottle, lab/tank storage, or tris batch did not have statistically significant ( $p$ -  
301 value  $< 0.05$ ) correlations with the pH change of tris ( $p$ -values 0.12, 0.11 and 0.09, respectively). The results of the  
302 ANOVA support that tris can be held in bag type 1 or 2 and stored in a lab or tank and the pH will change similarly  
303 regardless of storage method for up to 300 days. Additional bag types could be tested, such as bags made by Pollution  
304 Measurement Corp. used by Lai et al. (2018) or Scholle DuraShield used by Takeshita et al. (2015).

305 These results suggest that when bags are carefully handled prior to and after filling, tris pH changes are small  
306 over time. Specific recommendations for further work include: bags must be handled with care and enclosed in  
307 protective containers to prevent damage, bags must be rinsed with tris prior to filling, and additional testing is merited  
308 to determine sources of and methods to reduce contamination, such as acid washing.

309 **4. Conclusions**

310 This article describes our characterization of the stability of tris buffer in artificial seawater when stored in  
311 purportedly gas-impermeable bags. Several different tests, initiated over the course of a year and a half and lasting up  
312 to 300 days, exhibited an average decrease of 5.8 mpH yr<sup>-1</sup>. In comparison, tris stored in standard borosilicate bottles  
313 was shown to have a decrease of 3.0 mpH yr<sup>-1</sup>. For yearlong deployments, an expected pH change of -0.0058 is well  
314 below the weather quality threshold of 0.02 pH units. This low rate of change demonstrates the value of bagged tris  
315 for in situ validation of autonomous pH sensors (regardless of sensor operating principles), particularly in highly  
316 dynamic areas where repeatability of calibration based on discrete samples is challenging. Given the thorough  
317 characterization of tris over wide ranges of environmental variables, this contribution can aid in the traceability and  
318 intercomparability of pH sensor measurements. While valuable at the current stage of development (as demonstrated  
319 by, e.g., Lai et al. (2018) and Bresnahan et al. (2021)), further development would ideally result in a commercially  
320 available bag and filling procedure that can yield a rate of pH change less than the climate threshold of 0.003 per year.  
321 This will require further tests to identify the source of CO<sub>2</sub>, gas exchange or microbial respiration, as well as steps to  
322 reduce or eliminate these sources.

323 Periodic measurement of bagged tris in situ would allow for detection of sensor drift. Most in situ pH sensors  
324 are deployed in the euphotic zone in coastal areas, typically resulting in expedited biofouling and sedimentation, and  
325 leading to sensor drift (Bresnahan et al., 2014) that could be identified and potentially corrected. Such periodic  
326 calibration/validation would aid in identifying sensor issues and allow for greater consistency and continuity between  
327 a timeseries and planned or vicarious crossovers where an automated calibration can be used to augment or replace  
328 pre- and post-deployment calibrations/validations.

329 Appendix A

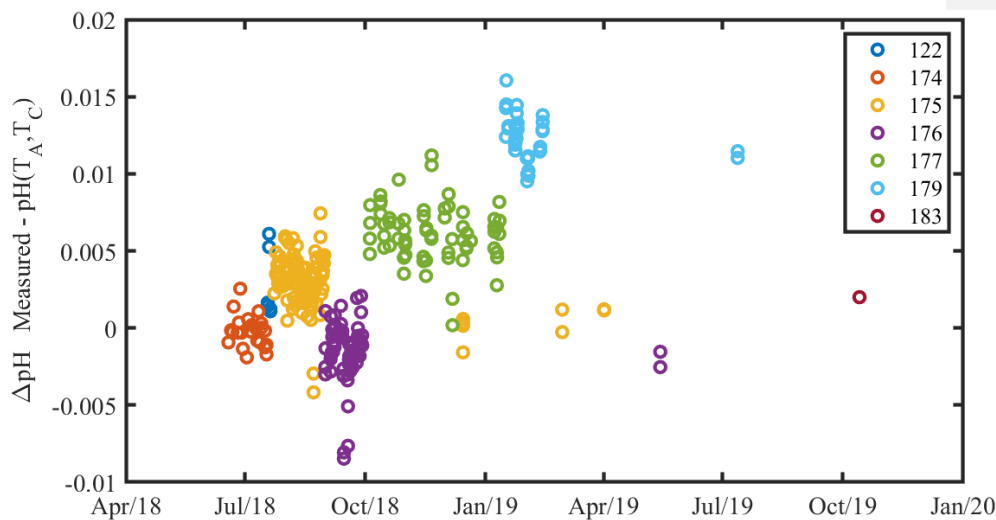
330

331 Table A1. Detailed information about the specific reagents used to make the tris solution. \*Reagent chemicals that meet or  
 332 surpass specifications of the British Pharmacopoeia (BP), European Pharmacopoeia (EP), Food Chemicals Codex (FCC),  
 333 United States Pharmacopoeia (USP).

334

Chemical	Manufacture	Part Number	Lot Number	Batch	Assay	Grade
tris	Fisher Scientific	T395-1	170360	all	99.8%	Certified ACS
NaCl	Fisher Scientific	S641-212	127252	all	99.0 to 100.5%	*BP/EP/FCC/USP
Na <sub>2</sub> SO <sub>4</sub>	Fisher Scientific	S421-1	134837	all	99.8%	Certified ACS
KCl	Fisher Scientific	P217-500	174416	all	99.7%	Certified ACS
MgCl <sub>2</sub>	Teknova	M0304	M030427E1401	all	1 M	Biotechnology
CaCl <sub>2</sub>	Amresco	E506-500mL	0982C098	all	0.95-1.05 M	Biotechnology
HCl	Fisher Scientific	SA48-1	175004	1, 2, 3	0.999 N	Certified
HCl	Fisher Scientific	SA48-1	188768	4	1.003 N	Certified

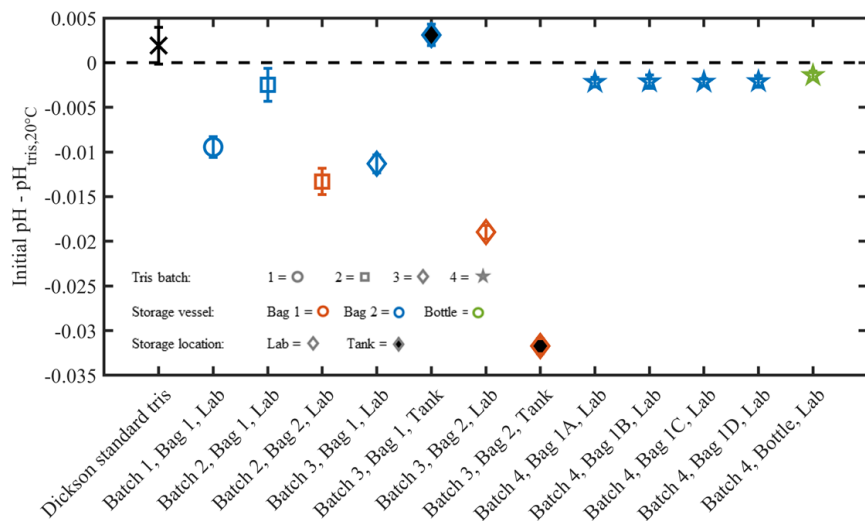
335



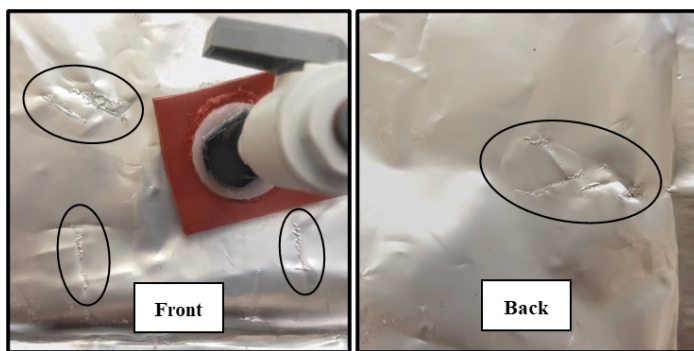
336

337 Fig. A1: A timeseries of the residual between measured and calculated CRM pH throughout the experiment. Marker color  
 338 denotes CRM batch number. There is a clear variability between measured and calculated pH, which is typical of CRM  
 339 batches (Andrew Dickson, *pers. comm.*). There was no observable systematic drift in the pH system during the experiment.  
 340 The mean standard deviation of pH measurements within a CRM batch is 0.0016, which is comparable to the 0.0019  
 341 reported in Bockmon & Dickson (2015). The same 760 nm absorbance wavelength outlier removal procedure used for tris  
 342 measurements was applied to CRM measurements.

343



344  
 345 Fig. A2: The initial pH residual of each tris bag or bottle measured in this experiment. The initial pH is reported as a  
 346 residual from the calculated pH at 20 °C. The initial pH was measured directly for tris batch 4 and extrapolated for tris  
 347 batches 1-3. Additionally, 2 bottles of Dickson standard tris (show by the black “X”) were measured on 12/10/2018. The  
 348 zero black dashed line is the calculated pH of tris at 20 °C, based upon the measured reagent concentrations (DeValls and  
 349 Dickson, 1998).



350  
 351 Fig. A3. The ovals indicate marks on the exterior of “Batch 2, Bag 1, Lab”. These marks appear to be damage to the interior  
 352 metallic layer, possibly due to creasing of the bag. These marks were not present on any other bag used in this study.

353  
 354

355 **Author contribution**

356 WW performed formal analysis, visualization, and writing – original draft preparation. KS and TW contributed  
357 to investigation and writing – review & editing. PB, YT, and TM contributed to funding acquisition, conceptualization,  
358 formal analysis, and writing – review & editing.

359 **Competing interests**

360 The authors declare that they have no conflict of interest.

361 **Data availability**

362 pH and  $C_T$  data are available via the UC San Diego Library Digital Collections at  
363 <https://doi.org/10.6075/J0QC022G> (Wolfe et al., 2021).

364 **Acknowledgements**

365 We thank May-Linn Paulsen and Andrew Dickson’s laboratory for sharing their tris expertise throughout this  
366 project. We thank the National Science Foundation Ocean Technology and Interdisciplinary Coordination (NSF-OTIC  
367 1736905 and NSF-OTIC 1736864) and the David and Lucile Packard Foundation for supporting this work.

368 **References**

- 369 ACT: Protocols for the Performance Verification of In Situ pH Sensors, Alliance for Coastal Technologies,  
370 <https://doi.org/10.25607/OBP-331>, 2012.
- 371 Aßmann, S., Frank, C., and Kortzinger, A.: Spectrophotometric high-precision seawater pH determination for use in  
372 underway measuring systems, *Ocean Sci.*, 7, 597-607, <https://doi.org/10.5194/os-7-597-2011>, 2011.
- 373 Bandstra, L., Hales, B., and Takahashi, T.: High-frequency measurements of total CO<sub>2</sub>: Method development and first  
374 oceanographic observations, *Mar. Chem.*, 100, 24-38, <https://doi.org/10.1016/j.marchem.2005.10.009>, 2006.
- 375 Bates, N., Astor, Y., Church, M., Currie, K., Dore, J., Gonzalez-Davila, M., Lorenzoni, L., Muller-Karger, F.,  
376 Olafsson, J., and Santana-Casiano, J.: A Time-Series View of Changing Surface Ocean Chemistry Due to  
377 Ocean Uptake of Anthropogenic CO<sub>2</sub> and Ocean Acidification, *J. Oceanogr.*, 27, 126-141,  
378 <https://doi.org/10.5670/oceanog.2014.16>, 2014.
- 379 Bittig, H. C., Steinhoff, T., Claustre, H., Fiedler, B., Williams, N. L., Sauzède, R., Kortzinger, A., and Gattuso, J.-P.:  
380 An Alternative to Static Climatologies: Robust Estimation of Open Ocean CO<sub>2</sub> Variables and Nutrient  
381 Concentrations From T, S, and O<sub>2</sub> Data Using Bayesian Neural Networks, *Front. Mar. Sci.*, 5,  
382 <https://doi.org/10.3389/fmars.2018.00328>, 2018.
- 383 Bockmon, E. E., and Dickson, A. G.: An inter-laboratory comparison assessing the quality of seawater carbon dioxide  
384 measurements, *Mar. Chem.*, 171, 36-43, <https://doi.org/10.1016/j.marchem.2015.02.002>, 2015.
- 385 Branch, T. A., DeJoseph, B. M., Ray, L. J., and Wagner, C. A.: Impacts of ocean acidification on marine seafood,  
386 *Trends Ecol. Evol.*, 28, 178-186, <https://doi.org/10.1016/j.tree.2012.10.001>, 2013.
- 387 Bresnahan, P. J., Takeshita, Y., Wirth, T., Martz, T. R., Cyronak, T., Albright, R., Wolfe, K., Warren, J. K., and Mertz,  
388 K.: Autonomous in situ calibration of ion-sensitive field effect transistor pH sensors, *Limnology and  
389 Oceanography: Methods*, 19, 132-144, <https://doi.org/10.1002/lom3.10410>, 2021.
- 390 Bresnahan, P. J., Martz, T. R., Takeshita, Y., Johnson, K. S., and LaShomb, M.: Best practices for autonomous  
391 measurement of seawater pH with the Honeywell Durafet, *Methods Oceanogr.*, 9, 44-60,  
392 <https://doi.org/10.1016/j.mio.2014.08.003>, 2014.



393 Bushinsky, S. M., Takeshita, Y., and Williams, N. L.: Observing changes in ocean carbonate chemistry: our  
394 autonomous future, *Curr. Clim*, 5, 207-220, <https://doi.org/10.1007/s40641-019-00129-8>, 2019.

395 Byrne, R. H.: Measuring Ocean Acidification: New Technology for a New Era of Ocean Chemistry, *Environ. Sci.*  
396 *Technol.*, 48, 5352-5360, <https://doi.org/10.1021/es405819p>, 2014.

397 Carter, B., Radich, J., Doyle, H., and Dickson, A.: An automated system for spectrophotometric seawater pH  
398 measurements, *Limnol. Oceanogr. Methods*, 11, 16-27, <https://doi.org/10.4319/lom.2013.11.16>, 2013.

399 Carter, B. R., Feely, R. A., Williams, N. L., Dickson, A. G., Fong, M. B., and Takeshita, Y.: Updated methods for  
400 global locally interpolated estimation of alkalinity, pH, and nitrate, *Limnol. Oceanogr. Methods*, 16, 119-  
401 131, <https://doi.org/10.1002/lom3.10232>, 2018.

402 Chavez, F., Pennington, J. T., Michisaki, R., Blum, M., Chavez, G., Friederich, J., Jones, B., Herlien, R., Kieft, B.,  
403 Hobson, B., Ren, A., Ryan, J., Sevadjian, J., Wahl, C., Walz, K., Yamahara, K., Friederich, G., and Messié,  
404 M.: Climate Variability and Change: Response of a Coastal Ocean Ecosystem, *J. Oceanogr.*, 30, 128-145,  
405 <https://doi.org/10.5670/oceanog.2017.429>, 2017.

406 Cooley, S. R., and Doney, S. C.: Anticipating ocean acidification's economic consequences for commercial fisheries,  
407 *Environ. Res. Lett.*, 4, 8, <https://doi.org/10.1088/1748-9326/4/2/024007>, 2009.

408 DeGrandpre, M. D., Spaulding, R. S., Newton, J. O., Jaqueth, E. J., Hamblock, S. E., Umansky, A. A., and Harris, K.  
409 E.: Considerations for the measurement of spectrophotometric pH for ocean acidification and other studies,  
410 *Limnol. Oceanogr. Methods*, 12, 830-839, <https://doi.org/10.4319/lom.2014.12.830>, 2014.

411 DelValls, T., and Dickson, A.: The pH of buffers based on 2-amino-2-hydroxymethyl-1,3-propanediol ('tris') in  
412 synthetic sea water, *Deep Sea Res. Part I*, 45, 1541-1554, [https://doi.org/10.1016/S0967-0637\(98\)00019-3](https://doi.org/10.1016/S0967-0637(98)00019-3),  
413 1998.

414 Dickson, A. G.: pH buffers for sea-water media based on the total hydrogen-ion concentration scale, *Deep Sea Res.*  
415 *Part I*, 40, 107-118, [https://doi.org/10.1016/0967-0637\(93\)90055-8](https://doi.org/10.1016/0967-0637(93)90055-8), 1993.

416 Dickson, A. G.: Reference materials for oceanic CO<sub>2</sub> measurements, *J. Oceanogr.*, 14, 21-22, 2001.

417 Dickson, A. G., Sabine, C. L., and Christian, J. R.: Guide to Best Practices for Ocean CO<sub>2</sub> Measurements, ICES  
418 Special Publication 3, North Pacific Marine Science Organization, Sidney, British Columbia, 191 pp., 2007.

419 Doney, S. C., Fabry, V. J., Feely, R. A., and Kleypas, J. A.: Ocean acidification: the other CO<sub>2</sub> problem, *Annu. Rev.*  
420 *Mar. Science*, 1, 169-192, <https://doi.org/10.1146/annurev.marine.010908.163834>, 2009.

421 Doney, S. C., Busch, D. S., Cooley, S. R., and Kroeker, K. J.: The impacts of ocean acidification on marine ecosystems  
422 and reliant human communities, *Annu. Rev. Environ. Resour.*, 45, <https://doi.org/10.1146/annurev-environ-012320-083019>, 2020.

424 Friederich, G., Walz, P., Bureczynski, M., and Chavez, F.: Inorganic carbon in the central California upwelling system  
425 during the 1997-1999 El Niño-La Niña event, *Prog. Oceanogr.*, 54, 185-203, [https://doi.org/10.1016/S0079-6611\(02\)00049-6](https://doi.org/10.1016/S0079-6611(02)00049-6), 2002.

426 Hales, B., Takahashi, T., and Bandstra, L.: Atmospheric CO<sub>2</sub> uptake by a coastal upwelling system, *Global*  
427 *Biogeochem. Cycles*, 19, <https://doi.org/10.1029/2004gb002295>, 2005.

429 Johnson, K. S., Jannasch, H. W., Coletti, L. J., Elrod, V. A., Martz, T. R., Takeshita, Y., Carlson, R. J., and Connery,  
430 J. G.: Deep-Sea DuraFET: A Pressure Tolerant pH Sensor Designed for Global Sensor Networks, *Anal.*  
431 *Chem.*, 88, 3249-3256, <https://doi.org/10.1021/acs.analchem.5b04653>, 2016.

432 Johnson, K. S., Plant, J. N., Coletti, L. J., Jannasch, H. W., Sakamoto, C. M., Riser, S. C., Swift, D. D., Williams, N.  
433 L., Boss, E., Haëntjens, N., Talley, L. D., and Sarmiento, J. L.: Biogeochemical sensor performance in the  
434 SOCCOM profiling float array, *J. Geophys. Res.: Oceans*, 122, 6416-6436,  
435 <https://doi.org/10.1002/2017jc012838>, 2017.

436 Karl, D. M.: Oceanic ecosystem time-series programs: Ten lessons learned, *J. Oceanogr.*, 23, 104-125,  
437 <https://doi.org/10.5670/oceanog.2010.27>, 2010.

438 Lai, C.-Z., DeGrandpre, M. D., and Darlington, R. C.: Autonomous Optofluidic Chemical Analyzers for Marine  
439 Applications: Insights from the Submersible Autonomous Moored Instruments (SAMI) for pH and pCO<sub>2</sub>,  
440 *Front. Mar. Sci.*, 4, <https://doi.org/10.3389/fmars.2017.00438>, 2018.

441 Liu, X. W., Patsavas, M. C., and Byrne, R. H.: Purification and Characterization of meta-Cresol Purple for  
442 Spectrophotometric Seawater pH Measurements, *Environ. Sci. Technol.*, 45, 4862-4868,  
443 <https://doi.org/10.1021/es200665d>, 2011.

444 Martz, T. R., Daly, K. L., Byrne, R. H., Stillman, J. H., and Turk, D.: Technology for ocean acidification research  
445 needs and availability, *J. Oceanogr.*, 28, 40-47, <https://doi.org/10.5670/oceanog.2015.30>, 2015.

446 McLaughlin, K., Dickson, A., Weisberg, S. B., Coale, K., Elrod, V., Hunter, C., Johnson, K. S., Kram, S., Kudela, R.,  
447 Martz, T., Negrey, K., Passow, U., Shaughnessy, F., Smith, J. E., Tadesse, D., Washburn, L., and Weis, K.

448 R.: An evaluation of ISFET sensors for coastal pH monitoring applications, *Reg. Stud. Mar. Sci.*, 12, 11-18,  
449 <https://doi.org/10.1016/j.rsma.2017.02.008>, 2017.

450 Müller, J., Bastkowski, F., Sander, B., Seitz, S., Turner, D., Dickson, A., and Rehder, G.: Metrology for pH  
451 Measurements in Brackish Waters-Part 1: Extending Electrochemical pH(T) Measurements of TRIS Buffers  
452 to Salinities 5-20, *Front. Mar. Sci.*, 5, <https://doi.org/10.3389/fmars.2018.00176>, 2018.

453 Müller, J. D., and Rehder, G.: Metrology of pH Measurements in Brackish Waters—Part 2: Experimental  
454 Characterization of Purified meta-Cresol Purple for Spectrophotometric pH(T) Measurements, *Front. Mar.  
455 Sci.*, 5, 177, <https://doi.org/10.3389/fmars.2018.00177>, 2018.

456 Nemzer, B., and Dickson, A.: The stability and reproducibility of Tris buffers in synthetic seawater, *Mar. Chem.*, 96,  
457 237-242, <https://doi.org/10.1016/j.marchem.2005.01.004>, 2005.

458

459 Newton, J., Feely, R., Jewett, E., Williamson, P., and Mathis, J.: *Global Ocean Acidification Observing Network:  
460 Requirements and Governance Plan. Second Edition*, 2015.

461 O'Sullivan, D. W., and Millero, F. J.: Continual measurement of the total inorganic carbon in surface seawater, *Mar.  
462 Chem.*, 60, 75-83, [https://doi.org/10.1016/s0304-4203\(97\)00079-0](https://doi.org/10.1016/s0304-4203(97)00079-0), 1998.

463 Okazaki, R. R., Sutton, A. J., Feely, R. A., Dickson, A. G., Alin, S. R., Sabine, C. L., Bunje, P. M. E., and Virmani,  
464 J. I.: Evaluation of marine pH sensors under controlled and natural conditions for the Wendy Schmidt Ocean  
465 Health XPRIZE, *Limnol. Oceanogr. Methods*, 15, 586-600, <https://doi.org/10.1002/lom3.10189>, 2017.

466 Paulsen, M. L., and Dickson, A. G.: Preparation of 2-amino-2-hydroxymethyl-1, 3-propanediol (TRIS) pHT buffers  
467 in synthetic seawater, *Limnol. Oceanogr. Methods*, 18, 504-515, <https://doi.org/10.1002/lom3.10383>, 2020.

468 Papadimitriou, S., Loucaides, S., Rérolle, V., Achterberg, E. P., Dickson, A. G., Mowlem, M., and Kennedy, H.: The  
469 measurement of pH in saline and hypersaline media at sub-zero temperatures: Characterization of Tris  
470 buffers, *Mar. Chem.*, 184, 11–20, <https://doi.org/10.1016/j.marchem.2016.06.002>, 2016.

471 Pierrot, D., Neill, C., Sullivan, K., Castle, R., Wanninkhof, R., Lüger, H., Johannessen, T., Olsen, A., Feely, R. A.,  
472 and Cosca, C. E.: Recommendations for autonomous underway pCO<sub>2</sub> measuring systems and data-reduction  
473 routines, *Deep Sea Res. Part II*, 56, 512-522, <https://doi.org/10.1016/j.dsr2.2008.12.005>, 2009.

474 Rodriguez, C., Huang, F., and Millero, F. J.: The partial molal volume and compressibility of Tris and Tris-HCl in  
475 water and 0.725 m NaCl as a function of temperature, *Deep Sea Res. Part I*, 104, 41-51,  
476 <https://doi.org/10.1016/j.dsr.2015.06.008>, 2015.

477 Sabine, C., Sutton, A., McCabe, K., Lawrence-Slavas, N., Alin, S., Feely, R., Jenkins, R., Maenner, S., Meinig, C.,  
478 and Thomas, J.: Evaluation of a new carbon dioxide system for autonomous surface vehicles, *J. Atmos.  
479 Oceanic Technol.*, 37, 1305-1317, <https://doi.org/10.1175/JTECH-D-20-0010.1>, 2020.

480 Sayles, F. L., and Eck, C.: An autonomous instrument for time series analysis of TCO<sub>2</sub> from oceanographic moorings,  
481 *Deep Sea Res. Part I*, 56, 1590-1603, <https://doi.org/10.1016/j.dsr.2009.04.006>, 2009.

482 Seidel, M. P., DeGrandpre, M. D., and Dickson, A. G.: A sensor for in situ indicator-based measurements of seawater  
483 pH, *Mar. Chem.*, 109, 18-28, <https://doi.org/10.1016/j.marchem.2007.11.013>, 2008.

484 Sloyan, B. M., Wanninkhof, R., Kramp, M., Johnson, G. C., Talley, L. D., Tanhua, T., McDonagh, E., Cusack, C.,  
485 O'Rourke, E., McGovern, E., Katsumata, K., Diggs, S., Hummon, J., Ishii, M., Azetsu-Scott, K., Boss, E.,  
486 Anson, I., Perez, F. F., Mercier, H., Williams, M. J. M., Anderson, L., Lee, J. H., Murata, A., Kouketsu, S.,  
487 Jeansson, E., Hoppema, M., and Campos, E.: The Global Ocean Ship-Based Hydrographic Investigations  
488 Program (GO-SHIP): A Platform for Integrated Multidisciplinary Ocean Sci., *Front. Mar. Sci.*, 6,  
489 <https://doi.org/10.3389/fmars.2019.00445>, 2019.

490 Spaulding, R. S., DeGrandpre, M. D., Beck, J. C., Hart, R. D., Peterson, B., De Carlo, E. H., Drupp, P. S., and Hammar,  
491 T. R.: Autonomous in Situ Measurements of Seawater Alkalinity, *Environ. Sci. Technol.*, 48, 9573-9581,  
492 <https://doi.org/10.1021/es501615x>, 2014.

493 Sutton, A. J., Feely, R. A., Maenner-Jones, S., Musielwicz, S., Osborne, J., Dietrich, C., Monacci, N., Cross, J., Bott,  
494 R., and Kozyr, A.: Autonomous seawater pCO<sub>2</sub> and pH time series from 40 surface buoys and the emergence  
495 of anthropogenic trends, *Earth Syst. Sci. Data*, 421, <https://doi.org/10.5194/essd-11-421-2019>, 2019.

496 Takeshita, Y., Frieder, C. A., Martz, T. R., Ballard, J. R., Feely, R. A., Kram, S., Nam, S., Navarro, M. O., Price, N.  
497 N., and Smith, J. E.: Including high-frequency variability in coastal ocean acidification projections,  
498 *Biogeosciences*, 12, 5853-5870, <https://doi.org/10.5194/bg-12-5853-2015>, 2015.

499 Takeshita, Y., McGillis, W., Briggs, E. M., Carter, A. L., Donham, E. M., Martz, T. R., Price, N. N., and Smith, J. E.:  
500 Assessment of net community production and calcification of a coral reef using a boundary layer approach,  
501 *J. Geophys. Res.: Oceans*, 121, 5655-5671, <https://doi.org/10.1002/2016JC011886>, 2016.

502 Takeshita, Y., Martz, T. R., Coletti, L. J., Dickson, A. G., Jannasch, H. W., and Johnson, K. S.: The effects of pressure  
503 on pH of Tris buffer in synthetic seawater, *Mar. Chem.*, 188, 1-5, <https://doi.org/10.1016/j.marchem.2016.11.002>,  
504 2017.

505 Takeshita, Y., Johnson, K. S., Martz, T. R., Plant, J. N., and Sarmiento, J. L.: Assessment of Autonomous pH  
506 Measurements for Determining Surface Seawater Partial Pressure of CO<sub>2</sub>, *J. Geophys. Res.: Oceans*, 123,  
507 4003-4013, <https://doi.org/10.1029/2017jc013387>, 2018.

508 Takeshita, Y., et al.: Consistency and stability of purified meta-cresol purple for spectrophotometric pH measurements  
509 in seawater, *Mar. Chem.*, in review.

510 Tilbrook, B., Jewett, E. B., DeGrandpre, M. D., Hernandez-Ayon, J. M., Feely, R. A., Gledhill, D. K., Hansson, L.,  
511 Isensee, K., Kurz, M. L., Newton, J. A., Siedlecki, S. A., Chai, F., Dupont, S., Graco, M., Calvo, E., Greeley,  
512 D., Kapsenberg, L., Lebrech, M., Pelejero, C., Schoo, K. L., and Telszewski, M.: An Enhanced Ocean  
513 Acidification Observing Network: From People to Technology to Data Synthesis and Information Exchange,  
514 *Front. Mar. Sci.*, 6, 21, <https://doi.org/10.3389/fmars.2019.00337>, 2019.

515 Wang, Z. A., Sonnichsen, F. N., Bradley, A. M., Hoering, K. A., Lanagan, T. M., Chu, S. N., Hammar, T. R., and  
516 Camilli, R.: In Situ Sensor Technology for Simultaneous Spectrophotometric Measurements of Seawater  
517 Total Dissolved Inorganic Carbon and pH, *Environ. Sci. Technol.*, 49, 4441-4449,  
518 <https://doi.org/10.1021/es504893n>, 2015.

519 Wang, Z. A., Moustahfid, H., Mueller, A. V., Michel, A. P. M., Mowlem, M., Glazer, B. T., Mooney, T. A., Michaels,  
520 W., McQuillan, J. S., Robidart, J. C., Churchill, J., Sourisseau, M., Daniel, A., Schaap, A., Monk, S.,  
521 Friedman, K., and Brehmer, P.: Advancing Observation of Ocean Biogeochemistry, Biology, and  
522 Ecosystems With Cost-Effective in situ Sensing Technologies, *Front. Mar. Sci.*, 6, 22,  
523 <https://doi.org/10.3389/fmars.2019.00519>, 2019.

524 Williams, N. L., Juranek, L. W., Johnson, K. S., Feely, R. A., Riser, S. C., Talley, L. D., Russell, J. L., Sarmiento, J.  
525 L., and Wanninkhof, R.: Empirical algorithms to estimate water column pH in the Southern Ocean, *Geophys.*  
526 *Res. Lett.*, 43, 3415-3422, <https://doi.org/10.1002/2016gl068539>, 2016.

527 Wolfe, W. H., Shipley, K. M., Bresnahan, P. J., Takeshita, Y., Wirth, T., Martz, T. R.: Data from: Technical note:  
528 stability of tris pH buffer in artificial seawater stored in bags. UC San Diego Library Digital  
529 Collections. <https://doi.org/10.6075/J0QC022G>, 2021.